Gradual Configuration Research on Energy Storage System for a Photovoltaic Plant

Haihong Bian[1], Wei Wang[2], Kai Chen[3], Xiaohui Xu[4], Qingshan Xu[2]
[1]*School of Electric Power Engineering, Nanjing Institute of Technology, Nanjing, Jiangsu, China, 211167*
[2]*School of Electrical Engineering, Southeast University, Nanjing, Jiangsu, China, 210096*
[3]*Nanjing Power Supply Company, Nanjing, Jiangsu, China, 210008*
[4]*China Electric Power Research Institute, Nanjing, Jiangsu, China, 210061*
bianhh.njit@gmail.com

***Abstract*—A gradual configuration research on energy storage system (ESS) is proposed and applied for photovoltaic (PV) plant in this paper. First, the ESS is used to absorb the unbalanced energy between the solar power generation and load demand. It is found that ESS capacity will be extremely large to meet all the balancing requirements. A simple solution for this problem is to allow excess power generation. Then, the ESS is installed at a PV plant to achieve generation schedule based on power forecast. A modified probabilistic approach is adopted to study the impact on the needs for storage because of the forecast errors. Results show that the required ESS capacity can be significantly reduced when a small amount of residual PV output uncertainty has been permitted. Lastly, to be more practical and economical, utilising the ESS for power fluctuations smoothing is also included in this study. It is shown that the ESS capacity is strongly influenced by the smoothness of the output wanted, but much smaller than the two situations mentioned above.**

***Index Terms*—Capacity selecting, discrete Fourier transform (DFT), energy storage system (ESS), fluctuation smoothing, photovoltaic plant.**

I. INTRODUCTION

The last decade has witnessed a rapid growth of the photovoltaic (PV) production all over the world. An increase of 48% each year on average since 2002 has made it the world's fastest growing energy technology [1]–[3]. PV electricity generation is highly desirable for remote areas due to the absence of mechanical parts, in case of non-sun trackers, long service lifetime, high reliability, and low maintenance requirements [4]. However, PV system has its disadvantages. The output of a PV system fluctuates depending on weather conditions, season and geographic location [5], which may cause problems [6]–[8]. The energy storage system (ESS) can be an excellent solution for these problems due to its ability of absorbing or releasing energy when necessary [9]–[13]. To maintain energy balance between energy production and consumption is a basic use of the ESS. Heide et al. [14] described the storage and balancing needs of hourly power mismatches between generation and load in a simplified European power system based on solar and wind power generation only. Kaushika et al. [15] investigated a stand-alone PV system with interconnected arrays for optimal sizing of the array and battery bank using the system simulation modelling, which considers the electricity generation in the array and its storage in the battery bank serving the fluctuating load demand and used the loss of power supply probability (LPSP) to connote the risk of not satisfying the load demand. To obtain an optimised operation of PV and battery system, the security-constrained unit commitment (SCUC) algorithm was applied to determine the hourly charge or discharge schedule of the battery in a large power system in [16].

Another important role of the ESS is to make the solar power systems more dispatchable. An appropriate capacity of the ESS is preferred if performance and economic cost are taken into account at the same time. Some publications dedicated to the research about the impacts on the ESS size of solar or wind power forecasts aiming to reduce the required capacity are in sight [17]–[19]. Kreikebaum et al. [20] quantified the level of energy storage and forecasting necessary to reduce the intra-hour variability of a PV plant, finding that more than a 90% cost reduction is required to justify deployment of a battery energy storage system. Nottrott et al. [21] used linear programming (LP) to leverage PV power output and load forecasts to minimize peak loads subject to elementary dynamical and electrical constraints of a combined photovoltaic-battery storage system. Further analysis was performed in [22] where the financial value of forecasting in energy storage dispatch optimization was calculated as a function of battery capacity ratio.

Due to the unfavourable influence of power fluctuations from PV plants and expensive cost of the ESS, extensive studies have been carried out on the power smoothing through

Manuscript received February 12, 2013; accepted May 4, 2013.
This research was funded by National High Technology Research and Development Program of China (863 Program) (No. 2012AA050214), Natural Science Foundation of Jiangsu Province (No. BK2012753), the Fundamental Research Funds for the Central Universities (3216002103) and National Energy Administration (NY20110702-1).

proper control of ESS [23]. In [23], a control method was presented for selecting the economically optimal battery capacity to reduce the frequency deviations of a stand-alone PV-based power system, which at the same time maintained the SOC within certain range to increase the lifetime of the battery. Woyte et al constructed a power smoothing model, based on wavelet theory, to determine the capacity of storage devices that would be necessary for mitigating voltage and power fluctuations introduced by photovoltaics. However, the choice for number of decomposition layers is somewhat arbitrary.

An appropriate ESS capacity, considering its high one-time investment, is crucial to the stable and economic operation of the system. This study will estimate the size of an ESS required to eliminate imbalance penalties and smooth power fluctuations when sited at a PV plant. Three typical modes are established and the corresponding method is introduced. Furthermore, influencing factors that affect the ESS capacity are also studied.

The other parts of this paper are organized as follows. Section II details the three modes and corresponding methods, Section III describes the data used for analysis, Section IV analyses the results and influencing factors, Section V draws the conclusions.

II. Modes and Methodology

In this section, three different modes are constructed and the corresponding methods for selecting the optimal ESS energy capacity are introduced.

A. Mode 1: ESS capacity as a function of excess PV power generation

If the unbalance between the generation and load is to be maintained, the needs for storage can be tremendous. A simple solution for this is to allow excess solar power generation. Hourly power mismatches, especially for negative ones, will decrease thus lowering the need for storage. In this mode, ESS is used to absorb the unbalance energy between power generation and load demand with excess solar power generation.

The hourly power mismatch can be written as

$$\Delta p(t) = (1+\alpha)P(t) - L(t), \tag{1}$$

where α is the average excess generation. When the mismatch is positive, the excess power is charged into the ESS with efficiency η_c. And for a negative one, the generation deficit will be supplied by the ESS with efficiency η_{dc}. A simple non-constrained storage model can be obtained

$$E(t) = E(t-1) + \begin{cases} \Delta p(t)\cdot\eta_c, \\ \Delta p(t)/\eta_{dc}. \end{cases} \tag{2}$$

The time series $E(t)$ describes the storage level the ESS. However, when on average power generation minus storage losses is bigger than load, the fluctuating storage level will drift in time. To solve this problem, a new method to calculate the ESS capacity is proposed in [14]

$$E = \max[E(t) - \min E(t)]. \tag{3}$$

At time t_0 the non-constrained ESS filling level is $E(t_0)$ and, in the following time $t \geq t_0$ the non-constrained storage level never drops below $\min\limits_{t\geq t_0} E(t)$. Their difference represents the energy needed from the ESS at time t_0. The maximum over all times leads to the required ESS capacity E_N for the whole year. Thus, a constrained storage-level time series are generated

$$E_{con}(t) = \begin{cases} E_{con}(t-1) + \Delta p(t)\cdot\eta_c, & \Delta p(t) \leq 0, \\ E_{con}(t-1) + \Delta p(t)/\eta_{dc}, & 0 < \Delta p(t) < (E_N - E_{con}(t-1))/\eta_c, \\ E_N, & \Delta p(t) > (E_N - E_{con}(t-1))/\eta_c. \end{cases} \tag{4}$$

Under constrained conditions, the storage level will not exceed the ESS capacity E_N obtained from (3) and, for a sufficiently large initial value $0 < E_{con}(0) < E_N$, never drop below zero. Whenever the constrained storage is full, the excess power is discarded. This is the main difference from the unconstrained storage model.

B. Mode 2: ESS capacity as a function of PV power generation forecast errors

In this part, ESS is installed to compensate forecast errors. A probabilistic method will be used for ESS sizing, whose core thought is to allow the remaining uncertainty termed unserved energy to a certain degree to observe the reduction of the required ESS capacity. An improvement of forecast method is performed based on the persistence approach

$$\hat{P}(t) = \frac{1}{N}[P(t-N) + P(t-N+1) + ... + P(t-1)], \tag{5}$$

where $\hat{P}(t)$ is the solar power forecast for time t, N is the number of time steps within prediction period T, $T = N\cdot\Delta t$, and Δt the time step length of the time series of solar power generation ($\Delta t = 1\text{h}$).

In the traditional persistence forecast model, the forecast is updated once per prediction period T and keeps constant during the whole period. Instead, for the modified forecast method used in this paper, the forecast is updated every hour. Thus, the forecast result can track the change trend of solar generation leading to an improvement of forecast quality. The forecast error ε is calculated as the difference between the solar power forecast $\hat{P}(t)$ and the measured solar power $P(t)$

$$\varepsilon(t) = \hat{P}(t) - P(t). \tag{6}$$

When $\varepsilon(t)$ is positive, it represents the power should be supplied by the ESS, and vice versa, absorbed. The unserved energy is put forward to calculate the energy that cannot be

compensated by the ESS.

The unserved energy may be estimated by:

$$e_{\text{ue}} \approx ETR \cdot t_{sat}, \tag{7}$$

$$ETR = \frac{E_{\text{tp}}}{E_{\text{total}}}. \tag{8}$$

In (7), *ETR* is the energy throughput ratio and t_{sat} the saturation time which describes the level of compensation. In (8), E_{tp} is the absolute energy that ESS charged and discharged summed up, and E_{total} the total generated energy.

Based on forecast error, time series of E(t), the storage level of a non-constrained ESS, can be obtained. The storage efficiency is assumed to be 100% here. A zero-error situation e'_{s0} represents an ESS with enough energy capacity to compensate any difference from the forecast. Considering the negative values of E(t) do not make any sense, a new definition is introduced and expressed as follows

$$e_{s0} = \max_t E(t) - \min_t E(t). \tag{9}$$

At the same time, the practical storage level of ESS is $E'(t) = E(t) - \min_t E(t)$.

The saturation time t_{sat} can be obtained from the cumulative distribution function (CDF) of $E'(t)$. According to the definition of CDF, the cumulative frequency f_{SOC} of any value of $E'(t)$ represents the percentage of time that the storage level will be below this value. If, for example, ESS capacity is reduced to E_{x}, $100 - f_{soc}(E_x)$ is the time the storage level will be larger than E_{x}, which is the so-called saturation time t_{sat}

$$t_{sat} = 100 - f_{soc}(E_x). \tag{10}$$

In case of different distribution shapes of $E'(t)$, a saturation time splitting coefficient, c_s, is introduced and thus a more practical method can be expressed as

$$E_{\text{ESS}} = \min_{c_s}[f_{soc}^{-1}(100 - c_s t_{sat}) - f_{soc}^{-1}((1 - c_s)t_{sat})], \tag{11}$$

where EESS is the minimized ESS capacity needed for a certain saturation time t_{sat}, f_{soc}^{-1} is the inverted cumulative distribution function of $E'(t)$, and c_s the saturation time splitting coefficient, $0 \le c_s \le 1$.

C. Mode 3: ESS capacity as a function of power maximum fluctuation rate

In this Mode, ESS is used to smooth the power fluctuation of PV plant output. A spectrum analysis of the solar power sample is carried out in this part based on Discrete Fourier Transform (DFT), aiming to divide the analysed power sample into the high-frequency and low-frequency part. The high-frequency part is absorbed by the ESS and the low-frequency part is the smoothed output of the photovoltaic plant. The main thought of the method adopted here is to decide the minimized compensated frequency range by the ESS to make the output smooth enough to connect to the grid. Thus, the optimal ESS size can be obtained within the following steps.

Step 1. Perform Discrete Fourier Transform to the solar power sample.

The result can be expressed as

$$\begin{cases} \boldsymbol{S}_g = F(P_g) = [S_g(1), ..., S_g(n), ..., S_g(N_s)]^{\text{T}} \\ \boldsymbol{f}_g = [f_g(1), ..., f_g(n), ..., f_g(N_s)]^{\text{T}} \end{cases}, \tag{12}$$

where $\boldsymbol{P}_g = [P_g(1), ..., P_g(n), ..., P_g(N_s)]^{\text{T}}$ is the analysed power sample, N_s is the sampling length, and $\boldsymbol{S}_g$, $\boldsymbol{f}_g$ the amplitude and frequency vector respectively. In particular, $S_{\text{g}}(n)=R_{\text{g}}(n)+jI_{\text{g}}(n)$ is the amplitude with corresponding to the nth frequency of $f_{\text{g}}(n)$, and $R_{\text{g}}(n)$, $I_{\text{g}}(n)$ the real part and the imaginary part, respectively.

According to the knowledge of DFT, $f_{\text{g}}(n)$ is calculated as follows

$$f_g(n) = \frac{f_s(n-1)}{N_s} = \frac{n-1}{T_s N_s}, \tag{13}$$

where f_{s}, T_{s} is the sampling frequency (Hz) and the sampling period (s), respectively. For more information about $\boldsymbol{S}_{\text{g}}$, it is a complex vector with Nyquist frequency ($f_{\text{Ny}}=f_{\text{s}}/2$, the highest frequency can be observed according to sampling theorem) as the axis of symmetry, and the symmetrical elements conjugate each other.

Step 2. Determine the minimized compensated frequency range by the ESS.

Assuming $\boldsymbol{f}_{\text{ps1}}$ is the determined compensated frequency range and $\boldsymbol{f}_{\text{ps2}}$ the symmetrical range with Nyquist frequency as the symmetry axis, the smoothed output can be obtained as the target output of the solar-battery system from (14) and (15):

$$S_c(n) = \begin{cases} 0 + j0, & f_n \in \boldsymbol{f}_{\text{ps1}} \cup \boldsymbol{f}_{\text{ps2}}, \\ S_g(n), & f_n \notin \boldsymbol{f}_{\text{ps1}} \cup \boldsymbol{f}_{\text{ps2}}, \end{cases} \tag{14}$$

$$\boldsymbol{P}_0 = F^{-1}(\boldsymbol{S}_c) = \left[P_0(1), ..., P_0(n), ..., P_0(N_s)\right]^{\text{T}}. \tag{15}$$

In (14), amplitudes of the elements within the compensated frequency range are set to zero, otherwise keep the same. In (15), F^{-1} represents Inverse Discrete Fourier Transform (IDFT).

To evaluate the compensation effect of ESS, maximum fluctuation rate (MFR) within time period T_{e} (10 min in this paper) is proposed

$$F_{T_{\text{e}}} = \frac{P_{T_{\text{e}}}^{\max} - P_{T_{\text{e}}}^{\min}}{P_{\text{N}}} \times 100\%, \tag{16}$$

where $P_{T_{\text{e}}}^{\max}$, $P_{T_{\text{e}}}^{\min}$ is, respectively, the maximum power and minimum power within T_{e}, and P_{N} the rated power.The aim of the ESS installation in this mode is nothing but reduce $F_{T_{\text{e}}}$ to an extent to meet the requirement of connecting the

photovoltaic plant to the grid.

Step 3. Obtain the optimal ESS size.

Based on the target output $\boldsymbol{P}_0$ generated in step 2, the ESS output can simply calculated as

$$P_{\mathrm{ESS0}}(n) = P_0(n) - P_{\mathrm{g}}(n). \tag{17}$$

When $P_{\mathrm{ESS0}}(n)$ is positive, the ESS should discharge, and vice versa. Considering the storage efficiency, a more practical output power of ESS is written as (18). Thus, a time series which describes the storage level of ESS can be generated in (19):

$$P_{\mathrm{ESS}}(n) = \begin{cases} \dfrac{P_{\mathrm{ESS0}}(n)}{\eta_{\mathrm{dc}}}, & P_{\mathrm{ESS0}}(n) \geq 0, \\ P_{\mathrm{ESS0}}(n)\eta_{\mathrm{c}}, & P_{\mathrm{ESS0}}(n) < 0, \end{cases} \tag{18}$$

$$E(m) = \sum_{0}^{m}\left(P_{\mathrm{ESS}}(m)\frac{T_{\mathrm{S}}}{3600}\right), \quad m = 0,1,..,N_s. \tag{19}$$

Furthermore, the energy balance has to be maintained, which means the energy supplied and absorbed by the ESS during its entire operating cycle (1d in this paper) should be equal to or close to zero. A correction has to be made to the target output $\boldsymbol{P}_0$ to compensate the storage losses. A simple method by lowering $\boldsymbol{P}_0$ is preferred here using trial and error method to determine how much to do this.

Based on the storage level $E(m)$, at the same time, taking care of the remaining capacity constraints, the optimal ESS size is obtained as

$$E_{\mathrm{ESS}} = \frac{\max E(m) - \min E(m)}{C_{\mathrm{up}} - C_{\mathrm{low}}}, \tag{20}$$

where C_{up}, C_{low} is the upper and lower limit of the remaining capacity respectively, $C_{up}, C_{low} \in [0, 1]$.

III. Data Illustration

According to the different roles of the ESS for a PV-based energy system in three modes, solar power output and load data of different time scales and resolution will be needed. All of the data used to size the ESS are obtained as follows (Fig. 1).

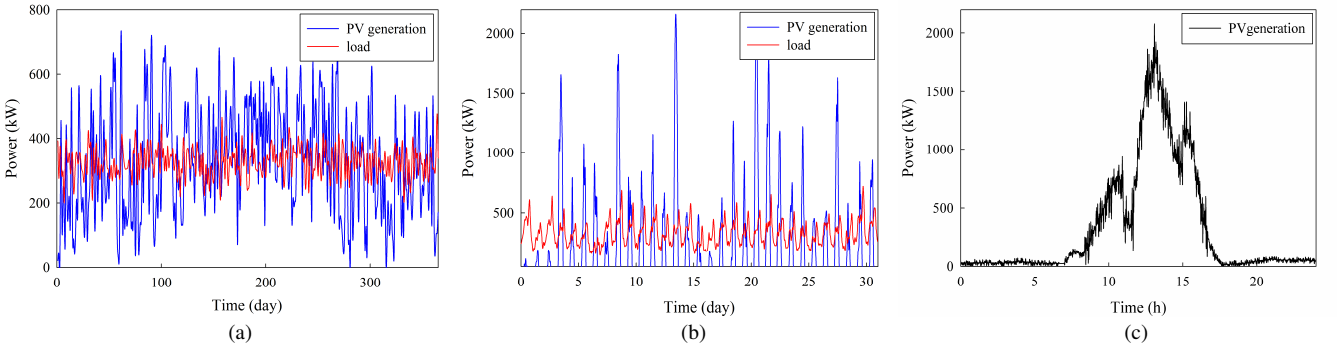

Fig. 1. PV generation and load (a) over one year with 1-day resolution, (b) over one arbitrary month with 1-h resolution, and (c) PV generation only over one day with 1-min resolution. In (a) and (b), load is scaled to the same yearly average of 327kW with PV generation power.

For Mode 1, and 2, long time scale data are required. We use TRNSYS (Version 16) to get typical meteorological year (TMY) solar radiation data of Shanghai, China. Then, another simulation software, HOMER, is applied, which provides a window to designate the latitude and the amount of solar radiation to generate the output data of the photovoltaic array for each hour of the year. Power rating of the PV plant analysed is set to 2.3 MW. At the same time, a typical hourly load profile is exported from HOMER. Complete spatial aggregation produces time series of the solar power generation $P(t)$ and load $L(t)$. Fig. 1 shows the whole year and an arbitrary one-month period situation, where $L(t)$ is scaled to the same yearly average of 327kW with $P(t)$.

In Mode 3, the ESS is installed for power fluctuation smoothing. In this part, solar power data with higher temporal resolution would be necessary. A time series of 1-min power output is generated based on a set of 5-second measured solar radiation data on February 25th and HOMER. In addition, to be more comparable with mode 1 and 2, it is also scaled to the same average of 327kW with $P(t)$. As has been seen in Fig. 1(c), a maximum fluctuation rate (MFR, see (16)) of 34.4% is observed.

IV. Results and Discussion

In Mode 1, an example of a constrained storage level time series is illustrated in Fig. 2. The required ESS capacity has a strong dependence on the excess generation α, which is illustrated in Fig. 3. As can be seen, the ESS capacity decreases fast with increasing α. For $\eta_c = \eta_{dc} = 1$, if 20% excess generation is permitted, energy capacity of the ESS can be reduced by more than 60%. For a 2.3-MW PV plant discussed in this paper, this leads to an ESS with 60 MWh, while for α=0, an installation with 160 MWh would be necessary. A continuous decrease of the required ESS capacity is observed if more excess generation is permitted. It is much more significant when the storage efficiencies is lower.

When $\eta_c = \eta_{dc} = 0.8$, for example, at α=0 the storage energy capacity E_{N} is 743 MWh, at α=0.15 E_{N} is half, and at α=0.32 it is a quarter. Note that when storage efficiency is lower than 1, some extra generation is needed to make up for the conversion losses, thus making the ESS size larger. It also shows that, according to Fig. 3, when α comes to 1 E_{N} is nearly 1.5% of annual load and almost independent of the storage efficiency.

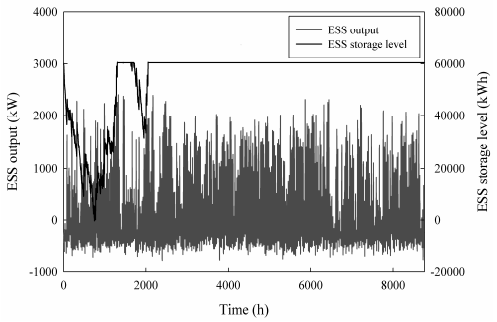

Fig. 2. ESS output power and storage level in a constrained model with α=0.2 and $\eta_c = \eta_{dc} = 0.1$.

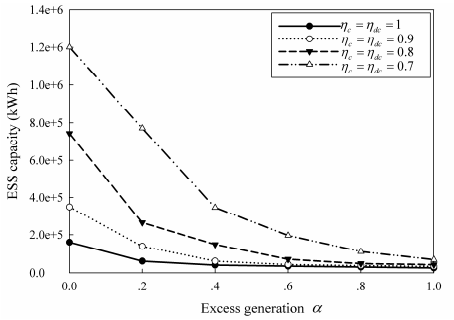

Fig. 3. ESS capacity as a function of excess generation α.

In Mode 2, the minimized ESS capacity for different forecast time periods T from 2 h up to 336 h (2 weeks) and for t_{sat} =0, 0.1, 1, 5, 10 and 25% are obtained based on the proposed probabilistic method. As shown in Fig. 4, the ESS size increases rapidly with T. The reason is that the predicted power curve will become smoother if T is larger, which leads to a decline in the forecast quality due to the loss of trend. It also can be seen from that *ETR* starts at about 0.2 and saturates near 1.1 when T comes to 24 h. This means a maximum of about 55% (energy charged or discharged is calculated twice, see (8)) of all generated energy would be cycled through the ESS. Fig. 5 shows the required ESS capacity as a function of unserved energy.

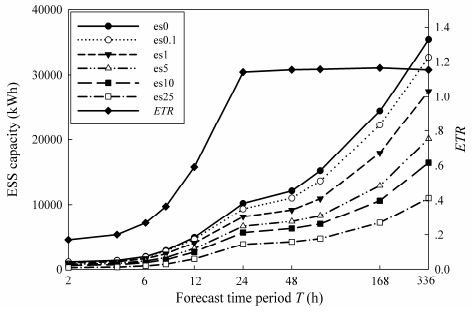

Fig. 4. *ETR* and ESS capacity as a function of forecast time period T. Here, es0 represents the ESS capacity with t_{sat}=0, and so on.

With 5% unserved energy permitted, a reduction of more than 60% ESS capacity is observed for T = 6 h, 50% for T = 12 h, and about 35% for T = 24, 48 h. The reduction degree declines when $T \le 24\text{h}$ and keeps stable basically when $T \ge 24\text{h}$. A possible reason for this is that for larger forecast time period T, a bigger *ETR* is obtained when $T \le 24\text{h}$ (Fig. 4) which leads to a decrease of e_{ue} according to (7). And for a certain e_{ue}, 5% here, the saturation time t_{sat} is reasonably smaller which can be a direct cause when the distribution shapes of the storage level are quite similar.

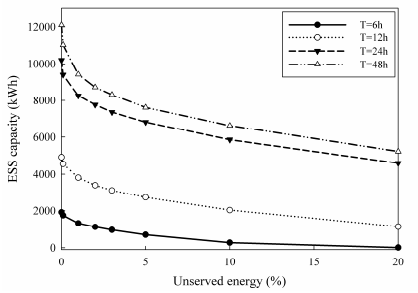

Fig. 5. ESS capacity as a function of unserved energy.

In Mode 3, the ESS size significantly depends on how smooth the compensated output is. Fig. 6 sees a basically stable decrease of the 10-min MFR with an increasing compensated frequency range. It also can be seen that the required ESS capacity grows slowly when the MFR is higher than 10%, and a dramatic increase in the capacity is observed if lower fluctuation rate is wanted. Taking storage efficiency into consideration, the distinguishing feature mentioned above keeps quite unchanged. An example of the smoothed power output with a MFR of 10% is given in Fig. 7. It should be pointed out that the combined output of the PV plant and ESS, sometimes, is below zero. It means the ESS will absorb power from the grid to charge itself to maintain energy balance, which is apparently unnecessary in the actual running process. It is a defect of the proposed method, and will be more significant when the compensated frequency range is larger.

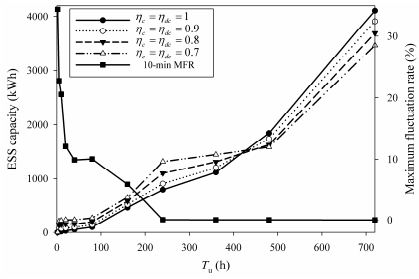

Fig. 6. ESS capacity and maximum fluctuation rate as a function of compensated frequency range. The compensated frequency range of [f_u, f_{Ny}] is transformed to [T_{Ny}, T_u] to be more observable, where f_{Ny} is the Nyquist frequency, T_u=1/f_u, T_{Ny}=1/f_{Ny}. The remaining capacity limits have been set C_{up}=0.5, C_{low}=0.95.

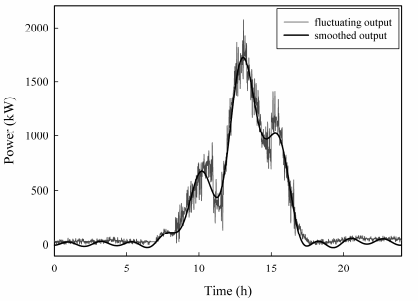

Fig. 7. Smoothed output of the PV system with a MFR of 10%.

The three modes are established for ESS sizing from different aspects and time scales. In Mode 1 the ESS is used to balance the solar power generation and load demand over the whole year. The ESS capacity determined is large enough to meet all the requirements in any situation thus making it the biggest one of the ESS sizes determined in the three modes. Mode 2 describes the impact of solar power forecast errors on the ESS size based on the probabilistic tool aiming to make

the PV plant more dispatchable. The ESS capacity is selected to be efficient in most cases (up to the unserved energy permitted) and it is the middle size. From a more operating perspective, the ESS is installed to make the PV plant output smoother in Mode 3. Its capacity is the smallest, but at the same time, more manipulation and possesses would be necessary. Table I shows the representative selecting results of the ESS capacity for a 2.3-MW PV plant in three modes, where an excess generation of 20% is permitted with $\eta_c = \eta_{dc} = 1$ in Mode 1, the unserved energy is set to 5% for T = 24 h in Mode 2, and a 10-min MFR of 10% is wanted with $\eta_c = \eta_{dc} = 1$ in Mode 3.

TABLE I. REPRESENTATIVE SELECTING RESULTS OF THE ESS CAPACITY IN THREE MODES.

Mode	Mode 1	Mode 2	Mode 3
ESS capacity	60376 kWh	6805kWh	96kWh

V. CONCLUSIONS

In this paper, three modes are constructed to select the ESS size for a PV plant from different aspects. Several conclusions can be derived from this study.

– The ESS capacity will be very large if all the unbalanced energy between power solar generation and load has to be maintained. Allowing excess power generation can be a simple solution.

– Further work can be done about the impact on the required ESS size of correlation between the power and load.

– Forecast quality has an important impact on the required ESS capacity. Permitting a spot of forecast error, the need for ESS capacity is significantly reduced.

– The ESS capacity lays a strong dependence on the smoothness of the combined output of PV system and ESS.

– Using DFT can conveniently and flexibly determine the ESS capacity according to the required maximum fluctuation rate which is more appropriate for large PV plant ESS sizing.

REFERENCES

[1] M. Olken, "The rise of the sun", *IEEE Power Energy*, vol. 7, no. 3, pp. 4, 2009. [Online]. Available: http://dx.doi.org/10.1109/MPE.2009.932311

[2] Q. S. Xu, N. C. Wang, K. Yukita, Y. Goto, K. Ichiyanagi, "Developed Modeling and Numerical Simulation for Mismatching Photovoltaic Performance Evaluation", *IEEJ Transactions on Electrical and Electronic Engineering*, vol. 4, pp. 545–552, 2009. [Online]. Available: http://dx.doi.org/10.1002/tee.20441

[3] H. X. Zang, Q. S. Xu, H. H. Bian, "Generation of typical solar radiation data for different climates of China", *Energy*, vol. 38, pp. 236–248, 2012. [Online]. Available: http://dx.doi.org/10.1016/j.energy.2011.12.008

[4] B. Wichert, "PV–diesel hybrid energy systems for remote area power generation – a review of current practice and future developments", *Renew. Sust. Energ. Rev.*, vol. 1, pp. 209–228, 1997. [Online]. Available: http://dx.doi.org/10.1016/S1364-0321(97)00006-3

[5] M. Datta, T. Senjyu, A. Yona, T. Funabashi, "Frequency Control of Photovoltaic–Diesel Hybrid System Connecting to Isolated Power Utility by Using Load Estimator and Energy Storage System", *IEEJ Transactions on Electrical and Electronic Engineering*, vol. 5, pp. 677–687, 2010. [Online]. Available: http://dx.doi.org/10.1002/tee.20592

[6] S. Yanagawa, T. Kato, K. Wu, A. Tabata, Y. Suzuoki, "Evaluation of LFC capacity for output fluctuation of photovoltaic generation systems based on multi–point observation of insolation", in *Proc. of IEEE Power Engineering Society Summer Meeting*, Vancouver, Canada, 2001, pp. 1652–1657.

[7] A. Woyte, V. V. Thong, R. Belmans, J. Nijs, "Voltage fluctuations on distribution level introduced by photovoltaic systems", *IEEE Trans. Energy Convers.*, vol. 21, no. 1, pp. 202–209, 2006. [Online]. Available: http://dx.doi.org/10.1109/TEC.2005.845454

[8] Y. Ruifeng, T. K. Saha, "Voltage Variation Sensitivity Analysis for Unbalanced Distribution Networks Due to Photovoltaic Power Fluctuations", *IEEE Transactions on Power Systems*, vol. 27, pp. 1078–1089, 2012. [Online]. Available: http://dx.doi.org/10.1109/TPWRS.2011.2179567

[9] W. A. Omran, M. Kazerani, M. Salama, "Investigation of Methods for Reduction of Power Fluctuations Generated From Large Grid–Connected Photovoltaic Systems", *IEEE Transactions on Energy Conversion*, vol. 26, pp. 318–327, 2011. [Online]. Available: http://dx.doi.org/10.1109/TEC.2010.2062515

[10] S. G. Tesfahunegn, O. Ulleberg, P. J. S. Vie, T. M. Undeland, "Optimal shifting of Photovoltaic and load fluctuations from fuel cell and electrolyzer to lead acid battery in a Photovoltaic/hydrogen standalone power system for improved performance and life time", *Journal of Power Sources*, vol. 196, pp. 10401–10414, 2011. [Online]. Available: http://dx.doi.org/10.1016/j.jpowsour.2011.06.037

[11] B. Azzopardi, "Integration of hybrid organic–based solar cells for micro–generation", Ph.D. dissertation, The University of Manchester, Manchester, UK, 2010.

[12] B. Azzopardi, J. Mutale, "Optimal integration of grid connected PV systems using emerging technologies", in *Proc. of 24th European Photovoltaic Solar Energy Conference*, Hamburg, Germany, 2009, pp. 3161–3166.

[13] B. Azzopardi, J. Mutale, 'Smart integration of future grid–connected PV systems', in *Proc. of 34th IEEE Photovoltaic Specialists Conference (PVSC)*, Philadelphia, United States, 2009, pp. 002364–002369. [Online]. Available: http://dx.doi.org/10.1109/PVSC.2009.5411318

[14] D. Heide, M. Greiner, L. von Bremend, C. Hoffmann, "Reduced storage and balancing needs in a fully renewable European power system with excess energy", *Renewable Energy*, pp. 2515–2523, 2011. [Online]. Available: http://dx.doi.org/10.1016/j.renene.2011.02.009

[15] N. D. Kaushika, N. K. Gautam, K. Kaushik, "Simulation model for sizing of stand – alone solar PV system with interconnected array", *Solar Energy Materials and Solar Cells*, vol. 85, pp. 499–519, 2005. [Online]. Available: http://dx.doi.org/10.1016/j.solmat.2004.05.024

[16] L. Bo, M. Shahidehpour, "Short–term scheduling of battery in a grid–connected PV/battery system", *IEEE Transactions on Power Systems*, vol. 20, no. 2, pp. 1053–1061, 2005. [Online]. Available: http://dx.doi.org/10.1109/TPWRS.2005.846060

[17] Y. Goto, T. Suzuki, T. Shimoo, T. Hayashi, S. Wakao, "Operation design of PV system with storage battery by using next–day residential load forecast", in *Proc. of 2011 37th IEEE Photovoltaic Specialists Conference (PVSC),* Seattle, United States, 2011, pp. 2369–2374.

[18] K. Bandara, T. Sweet, J. Ekanayake, "Photovoltaic applications for off–grid electrification using novel multi–level inverter technology with energy storage", *Renewable Energy*, vol. 37, pp. 82–88, 2012. [Online]. Available: http://dx.doi.org/10.1016/j.renene.2011.05.036

[19] R. Suzuki, Y. Hayashi, Y. Fujimoto, "Determination method of optimal planning and operation for residential PV system and storage battery based on weather forecast", in *Proc.* of *IEEE International Conference on Power and Energy (PECon),* Kota Kinabalu, Malaysia, 2012, pp. 343–347.

[20] F. Kreikebaum, R. Moghe, A. Prasai, D. Divan, "Evaluating the Application of Energy Storage and Day–Ahead Solar Forecasting to Firm the Output of a Photovoltaic Plant", in *Proc. of 2011 IEEE Energy Conversion Congress and Exposition (ECCE),* Phoenix, United States, 2011, pp. 3556–3561. [Online]. Available: http://dx.doi.org/10.1109/ECCE.2011.6064250

[21] A. Nottrott, J. Kleissl, B. Washom, "Storage dispatch optimization for grid–connected combined photovoltaic–battery storage systems", in *Proc. of IEEE Power And Energy Society General Meeting*, Vancouver, Canada, 2012, pp. 1–7. [Online]. Available: http://dx.doi.org/10.1109/PESGM.2012.6344979

[22] A. Nottrott, J. Kleissl, B. Washom, "Energy dispatch schedule optimization and cost benefit analysis for grid–connected, photovoltaic–battery storage systems", *Renewable Energy*, vol. 55, pp. 230–240, 2013. [Online]. Available: http://dx.doi.org/10.1016/j.renene.2012.12.036

[23] M. Datta, T. Senjyu, A. Yona, T. Funabashi, "Photovoltaic Output Power Fluctuations Smoothing by Selecting Optimal Capacity of Battery for a Photovoltaic–Diesel Hybrid System", *Electric Power Components and Systems*, vol. 39, pp. 621–644, 2011. [Online]. Available: http://dx.doi.org/10.1080/15325008.2010.536809